We are IntechOpen, the world's leading publisher of Open Access books Built by scientists, for scientists

4,800
Open access books available

122,000
International authors and editors

135M
Downloads

Our authors are among the

154
Countries delivered to

TOP 1%
most cited scientists

12.2%
Contributors from top 500 universities

CLARIVATE ANALYTICS BOOK CITATION INDEX INDEXED

WEB OF SCIENCE™

Selection of our books indexed in the Book Citation Index in Web of Science™ Core Collection (BKCI)

Interested in publishing with us?
Contact book.department@intechopen.com

Numbers displayed above are based on latest data collected.
For more information visit www.intechopen.com

Chapter 17

Theory of Ferromagnetic Unconventional Superconductors with Spin-Triplet Electron Pairing

Dimo I. Uzunov

Additional information is available at the end of the chapter

http://dx.doi.org/10.5772/48579

1. Introduction

In the beginning of this century the unconventional superconductivity of spin-triplet type had been experimentally discovered in several itinerant ferromagnets. Since then much experimental and theoretical research on the properties of these systems has been accomplished. Here we review the phenomenological theory of ferromagnetic unconventional superconductors with spin-triplet Cooper pairing of electrons. Some theoretical aspects of the description of the phases and the phase transitions in these interesting systems, including the remarkable phenomenon of coexistence of superconductivity and ferromagnetism are discussed with an emphasis on the comparison of theoretical results with experimental data.

The spin-triplet or p-wave pairing allows parallel spin orientation of the fermion Cooper pairs in superfluid ^{3}He and unconventional superconductors [1]. For this reason the resulting unconventional superconductivity is robust with respect to effects of external magnetic field and spontaneous ferromagnetic ordering, so it may coexist with the latter. This general argument implies that there could be metallic compounds and alloys, for which the coexistence of spin-triplet superconductivity and ferromagnetism may be observed.

Particularly, both superconductivity and itinerant ferromagnetic orders can be created by the same band electrons in the metal, which means that spin-1 electron Cooper pairs participate in the formation of the itinerant ferromagnetic order. Moreover, under certain conditions the superconductivity is enhanced rather than depressed by the uniform ferromagnetic order that can generate it, even in cases when the superconductivity does not appear in a pure form as a net result of indirect electron-electron coupling.

The coexistence of superconductivity and ferromagnetism as a result of collective behavior of f-band electrons has been found experimentally for some Uranium-based intermetallic compounds as, UGe_2 [2–5], URhGe [6–8], UCoGe [9, 10], and UIr [11, 12]. At low temperature ($T \sim 1$ K) all these compounds exhibit thermodynamically stable phase of coexistence of spin-triplet superconductivity and itinerant (f-band) electron ferromagnetism (in short, FS

phase). In UGe_2 and UIr the FS phase appears at high pressure ($P \sim 1$ GPa) whereas in URhGe and UCoGe, the coexistence phase persists up to ambient pressure (10^5Pa $\equiv$ 1bar).

Experiments, carried out in $ZrZn_2$ [13], also indicated the appearance of FS phase at $T < 1$ K in a wide range of pressures ($0 < P \sim 21$ kbar). In Zr-based compounds the ferromagnetism and the *p*-wave superconductivity occur as a result of the collective behavior of the *d*-band electrons. Later experimental results [14, 15] had imposed the conclusion that bulk superconductivity is lacking in $ZrZn_2$, but the occurrence of a surface FS phase at surfaces with higher Zr content than that in $ZrZn_2$ has been reliably demonstrated. Thus the problem for the coexistence of bulk superconductivity with ferromagnetism in $ZrZn_2$ is still unresolved. This raises the question whether the FS phase in $ZrZn_2$ should be studied by surface thermodynamics methods or should it be investigated by considering that bulk and surface thermodynamic phenomena can be treated on the same footing. Taking into account the mentioned experimental results for $ZrZn_2$ and their interpretation by the experimentalists [13–15] we assume that the unified thermodynamic approach can be applied. As an argument supporting this point of view let us mention that the spin-triplet superconductivity occurs not only in bulk materials but also in quasi-two-dimensional (2D) systems – thin films and surfaces and quasi-1D wires (see, e.g., Refs. [16]). In $ZrZn_2$ and UGe_2 both ferromagnetic and superconducting orders vanish at the same critical pressure P_c, a fact implying that the respective order parameter fields strongly depend on each other and should be studied on the same thermodynamic basis [17].

Fig. 1 illustrates the shape of the $T - P$ phase diagrams of real intermetallic compounds. The phase transition from the normal (N) to the ferromagnetic phase (FM) (in short, N-FM transition) is shown by the line $T_F(P)$. The line $T_{FS}(P)$ of the phase transition from FM to FS (FM-FS transition) may have two or more distinct shapes. Beginning from the maximal (critical) pressure P_c, this line may extend, like in $ZrZn_2$, to all pressures $P < P_c$, including the ambient pressure P_a; see the almost straight line containing the point 3 in Fig. 1. A second possible form of this line, as known, for example, from UGe_2 experiments, is shown in Fig. 1 by the curve which begins at $P \sim P_c$, passes through the point 2, and terminates at some pressure $P_1 > P_a$, where the superconductivity vanishes. These are two qualitatively different physical pictures: (a) when the superconductivity survives up to ambient pressure (type I), and (b) when the superconducting states are possible only at relatively high pressure (for UGe_2, $P_1 \sim 1$ GPa); type II. At the tricritical points 1, 2 and 3 the order of the phase transitions changes from second order (solid lines) to first order (dashed lines). It should be emphasized that in all compounds, mentioned above, $T_{FS}(P)$ is much lower than $T_F(P)$ when the pressure P is considerably below the critical pressure P_c (for experimental data, see Sec. 8).

In Fig. 1, the circle *C* denotes a narrow domain around P_c at relatively low temperatures ($T \lesssim 300$ mK), where the experimental data are quite few and the predictions about the shape of the phase transition are not reliable. It could be assumed, as in the most part of the experimental papers, that $(T = 0, P = P_c)$ is the zero temperature point at which both lines $T_F(P)$ and $T_{FS}(P)$ terminate. A second possibility is that these lines may join in a single (N-FS) phase transition line at some point $(T \gtrsim 0, P_c' \lesssim P_c)$ above the absolute zero. In this second variant, a direct N-FS phase transition occurs, although this option exists in a very small domain of temperature and pressure variations: from point $(0, P_c)$ to point $(T \gtrsim 0, P_c' \lesssim P_c)$. A third variant is related with the possible splitting of the point $(0, P_c)$, so that the N-FM line terminates at $(0, P_c)$, whereas the FM-FS line terminates at another zero temperature point

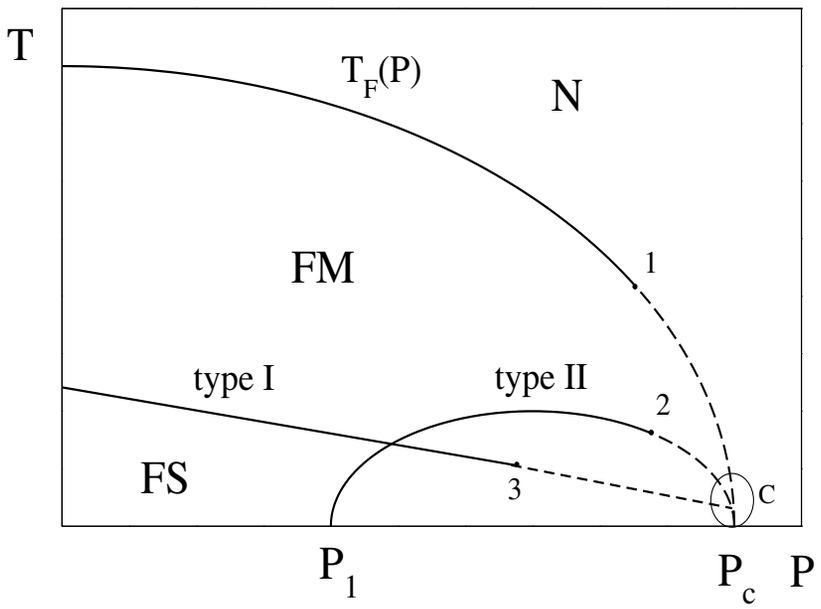

Figure 1. An illustration of $T-P$ phase diagram of p-wave ferromagnetic superconductors (details are omitted): N – normal phase, FM – ferromagnetic phase, FS – phase of coexistence of ferromagnetic order and superconductivity, $T_F(P)$ and $T_{FS}(P)$ are the respective phase transition lines: solid lines correspond to second order phase transitions, dashed lines stand for first order phase transition; 1 and 2 are tricritical points; P_c is the critical pressure, and the circle C surrounds a relatively small domain of high pressure and low temperature, where the phase diagram may have several forms depending on the particular substance. The line of the FM-FS phase transition may extend up to ambient pressure (type I ferromagnetic superconductors), or, may terminate at $T=0$ at some high pressure $P=P_1$ (type II ferromagnetic superconductors, as indicated in the figure).

$(0, P_{0c})$; $P_{0c} \lesssim P_c$. In this case, the p-wave ferromagnetic superconductor has three points of quantum (zero temperature) phase transitions [18, 19].

These and other possible shapes of $T-P$ phase diagrams are described within the framework of the general theory of Ginzburg-Landau (GL) type [18–20] in a conformity with the experimental data; see also Ref. [21]. The same theory has been confirmed by a microscopic derivation based on a microscopic Hamiltonian including a spin-generalized BCS term and an additional Heisenberg exchange term [22].

For all compounds, cited above, the FS phase occurs only in the ferromagnetic phase domain of the $T-P$ diagram. Particularly at equilibrium, and for given P, the temperature $T_F(P)$ of the normal-to-ferromagnetic phase (or N-FM) transition is never lower than the temperature $T_{FS}(P)$ of the ferromagnetic-to-FS phase transition (FM-FS transition). This confirms the point of view that the superconductivity in these compounds is triggered by the spontaneous magnetization $\boldsymbol{M}$, in analogy with the well-known triggering of the superfluid phase A_1 in ^{3}He at mK temperatures by the external magnetic field $\boldsymbol{H}$. Such "helium analogy" has been used in some theoretical studies (see, e.g., Ref. [23, 24]), where Ginzburg-Landau (GL) free energy terms, describing the FS phase were derived by symmetry group arguments. The non-unitary state, with a non-zero value of the Cooper pair magnetic moment, known from the theory of unconventional superconductors and superfluidity in ^{3}He [1], has been suggested firstly in Ref. [23], and later confirmed in other studies [7, 24]; recently, the same topic was comprehensively discussed in Ref. [25].

For the spin-triplet ferromagnetic superconductors the trigger mechanism was recently examined in detail [20, 21]. The system main properties are specified by terms in the GL expansion of form $M_i\psi_j\psi_k$, which represent the interaction of the magnetization $\boldsymbol{M} = \{M_j; j = 1, 2, 3\}$ with the complex superconducting vector field $\boldsymbol{\psi} = \{\psi_j; j = 1, 2, 3\}$. Particularly, these terms are responsible for the appearance of superconductivity ($|\boldsymbol{\psi}| > 0$) for certain T and P values. A similar trigger mechanism is familiar in the context of improper ferroelectrics [26].

A crucial feature of these systems is the nonzero magnetic moment of the spin-triplet Cooper pairs. As mentioned above, the microscopic theory of magnetism and superconductivity in non-Fermi liquids of strongly interacting heavy electrons (f and d band electrons) is either too complex or insufficiently developed to describe the complicated behavior in itinerant ferromagnetic compounds. Several authors (see [20, 21, 23–25]) have explored the phenomenological description by a self-consistent mean field theory, and here we will essentially use the thermodynamic results, in particular, results from the analysis in Refs. [20, 21]. Mean-field microscopic theory of spin-mediated pairing leading to the mentioned non-unitary superconductivity state has been developed in Ref. [17] that is in conformity with the phenomenological description that we have done.

The coexistence of s-wave (conventional) superconductivity and ferromagnetic order is a long-standing problem in condensed matter physics [27–29]. While the s-state Cooper pairs contain only opposite electron spins and can easily be destroyed by the spontaneous magnetic moment, the spin-triplet Cooper pairs possess quantum states with parallel orientation of the electron spins and therefore can survive in the presence of substantial magnetic moments. This is the basic difference in the magnetic behavior of conventional (s-state) and spin-triplet superconductivity phases. In contrast to other superconducting materials, for example, ternaty and Chevrel phase compounds, where the effect of magnetic order on s-wave superconductivity has been intensively studied in the seventies and eighties of last century (see, e.g., Refs. [27–29]), in these ferromagnetic compounds the phase transition temperature T_F to the ferromagnetic state is much higher than the phase transition temperature T_{FS} from ferromagnetic to a (mixed) state of coexistence of ferromagnetism and superconductivity. For example, in UGe_2 we have $T_{FS} \sim 0.8$ K versus maximal $T_F = 52$ K [2–5]. Another important difference between the ternary rare earth compounds and the intermetallic compounds (UGe_2, UCoGe, etc.), which are of interest in this paper, is that the experiments with the latter do not give any evidence for the existence of a standard normal-to-superconducting phase transition in zero external magnetic field. This is an indication that the (generic) critical temperature T_s of the pure superconductivity state in these intermetallic compounds is very low ($T_s \ll T_{FS}$), if not zero or even negative.

In the reminder of this paper, we present general thermodynamic treatment of systems with itinerant ferromagnetic order and superconductivity due to spin-triplet Cooper pairing of the same band electrons, which are responsible for the spontaneous magnetic moment. The usual Ginzburg-Landau (GL) theory of superconductors has been completed to include the complexity of the vector order parameter $\boldsymbol{\psi}$, the magnetization $\boldsymbol{M}$ and new relevant energy terms [20, 21]. We outline the $T - P$ phase diagrams of ferromagnetic spin-triplet superconductors and demonstrate that in these materials two contrasting types of thermodynamic behavior are possible. The present phenomenological approach includes both mean-field and spin-fluctuation theory (SFT), as the arguments in Ref. [30]. We propose

a simple, yet comprehensive, modeling of P dependence of the free energy parameters, resulting in a very good compliance of our theoretical predictions for the shape the $T-P$ phase diagrams with the experimental data (for some preliminary results, see Ref. [18, 19]).

The theoretical analysis is done by the standard methods of phase transition theory [31]. Treatment of fluctuation effects and quantum correlations [31, 32] is not included in this study. But the parameters of the generalized GL free energy may be considered either in mean-field approximation as here, or as phenomenologically renormalized parameters which are affected by additional physical phenomena, as for example, spin fluctuations.

We demonstrate with the help of present theory that we can outline different possible topologies for the $T-P$ phase diagram, depending on the values of Landau parameters, derived from the existing experimental data. We show that for spin-triplet ferromagnetic superconductors there exist two distinct types of behavior, which we denote as Zr-type (or, alternatively, type I) and U-type (or, type II); see Fig. 1. This classification of the FS, first mentioned in Ref. [18], is based on the reliable interrelationship between a quantitative criterion derived by us and the thermodynamic properties of the ferromagnetic spin-triplet superconductors. Our approach can be also applied to URhGe, UCoGe, and UIr. The results shed light on the problems connected with the order of the quantum phase transitions at ultra-low and zero temperatures. They also raise the question for further experimental investigations of the detailed structure of the phase diagrams in the high-P/low-T region.

2. Theoretical framework

Consider the GL free energy functional of the form

$$F(\boldsymbol{\psi},\boldsymbol{B})=\int_V d\boldsymbol{x}\left[f_{\mathrm{S}}(\boldsymbol{\psi})+f_{\mathrm{F}}(\boldsymbol{M})+f_{\mathrm{I}}(\psi,\boldsymbol{M})+\frac{\boldsymbol{B}^2}{8\pi}-\boldsymbol{B}.\boldsymbol{M}\right], \tag{1}$$

where the fields $\boldsymbol{\psi}$, $\boldsymbol{M}$, and $\boldsymbol{B}$ are supposed to depend on the spatial vector $\boldsymbol{x}\in V$ in the volume V of the superconductor. In Eq. (1), the free energy density generated by the generic superconducting subsystem ($\boldsymbol{\psi}$) is given by

$$f_{\mathrm{S}}(\boldsymbol{\psi})=f_{grad}(\boldsymbol{\psi})+a_s|\boldsymbol{\psi}|^2+\frac{b_s}{2}|\boldsymbol{\psi}|^4+\frac{u_s}{2}|\boldsymbol{\psi}^2|^2+\frac{v_s}{2}\sum_{j=1}^{3}|\psi_j|^4, \tag{2}$$

with

$$\begin{aligned} f_{grad}(\boldsymbol{\psi}) = {} & K_1(D_i\psi_j)^*(D_iD_j)+K_2\left[(D_i\psi_i)^*(D_j\psi_j)+(D_i\psi_j)^*(D_j\psi_i)\right] \\ & +K_3(D_i\psi_i)^*(D_i\psi_i), \end{aligned} \tag{3}$$

where a summation over the indices (i,j) is assumed, the symbol $D_j=(\hbar\partial/i\partial x_j+2|e|A_j/c)$ of covariant differentiation is introduced, and K_j are material parameters [1]. The free energy density $f_{\mathrm{F}}(\boldsymbol{M})$ of a standard ferromagnetic phase transition of second order [31] is

$$f_{\mathrm{F}}(\boldsymbol{M})=c_f\sum_{j=1}^{3}|\nabla\boldsymbol{M}_j|^2+a_f\boldsymbol{M}^2+\frac{b_f}{2}\boldsymbol{M}^4, \tag{4}$$

with $c_f, b_f > 0$, and $a_f = \alpha(T - T_f)$, where $\alpha_f > 0$ and T_f is the critical temperature, corresponding of the generic ferromagnetic phase transition. Finally, the energy $f_{\mathrm{I}}(\boldsymbol{\psi}, \boldsymbol{M})$ produced by the possible couplings of $\boldsymbol{\psi}$ and $\boldsymbol{M}$ is given by

$$f_{\mathrm{I}}(\boldsymbol{\psi}, \boldsymbol{M}) = i\gamma_0 \boldsymbol{M}.(\boldsymbol{\psi} \times \boldsymbol{\psi}^*) + \delta_0 \boldsymbol{M}^2 |\boldsymbol{\psi}|^2, \tag{5}$$

where the coupling parameter $\gamma_0 \sim J$ depends on the ferromagnetic exchange parameter $J > 0$, [23, 24] and δ_0 is the standard $\boldsymbol{M} - \boldsymbol{\psi}$ coupling parameter, known from the theory of multicritical phenomena [31] and from studies of coexistence of ferromagnetism and superconductivity in ternary compounds [27, 28].

As usual, in Eq. (2), $a_s = (T - T_s)$, where T_s is the critical temperature of the generic superconducting transition, $b_s > 0$. The parameters u_s and v_s and δ_0 may take some negative values, provided the overall stability of the system is preserved. The values of the material parameters $\mu = (T_s, T_f, \alpha_s, \alpha_f, b_s, u_s, v_s, b_f, K_j, \gamma_0$ and $\delta_0)$ depend on the choice of the substance and on intensive thermodynamic parameters, such as the temperature T and the pressure P. From a microscopic point of view, the parameters μ depend on the density of states $U_F(k_F)$ on the Fermi surface. On the other hand U_F varies with T and P. Thus the relationships $(T, P) \rightleftarrows U_F \rightleftarrows \mu$, i.e., the functional relations $\mu[U_F(T, P)]$, are of essential interest. While these relations are unknown, one may suppose some direct dependence $\mu(T, P)$. The latter should correspond to the experimental data.

The free energy (1) is quite general. It has been deduced by several reliable arguments. In order to construct Eq. (1)–(5) we have used the standard GL theory of superconductors and the phase transition theory with an account of the relevant anisotropy of the p-wave Cooper pairs and the crystal anisotropy, described by the u_s- and v_s-terms in Eq. (2), respectively. Besides, we have used the general case of cubic anisotropy, when all three components ψ_j of $\boldsymbol{\psi}$ are relevant. Note, that in certain real cases, for example, in UGe_2, the crystal symmetry is tetragonal, $\boldsymbol{\psi}$ effectively behaves as a two-component vector and this leads to a considerable simplification of the theory. As shown in Ref. [20], the mentioned anisotropy terms are not essential in the description of the main thermodynamic properties, including the shape of the $T - P$ phase diagram. For this reason we shall often ignore the respective terms in Eq. (2). The γ_0-term triggers the superconductivity ($\boldsymbol{M}$-triger effect [20, 21]) while the $\delta_0 \boldsymbol{M}^2 |\psi|^2$–term makes the model more realistic for large values of $\boldsymbol{M}$. This allows for an extension of the domain of the stable ferromagnetic order up to zero temperatures for a wide range of values of the material parameters and the pressure P. Such a picture corresponds to the real situation in ferromagnetic compounds [20].

The total free energy (1) is difficult for a theoretical investigation. The various vortex and uniform phases described by this complex model cannot be investigated within a single calculation but rather one should focus on particular problems. In Ref. [24] the vortex phase was discussed with the help of the criterion [33] for a stability of this state near the phase transition line $T_{c2}(\boldsymbol{B})$, ; see also, Ref. [34]. The phase transition line $T_{c2}(H)$ of a usual superconductor in external magnetic field $H = |\boldsymbol{H}|$ is located above the phase transition line T_s of the uniform (Meissner) phase. The reason is that T_s is defined by the equation $a_s(T) = 0$, whereas $T_{c2}(H)$ is a solution of the equation $|a_s| = \mu_B H$, where $\mu_B = |e|\hbar/2mc$ is the Bohr magneton [34]. For ferromagnetic superconductors, where $M > 0$, one should use the magnetic induction $\boldsymbol{B}$ rather than $\boldsymbol{H}$. In case of $\boldsymbol{H} = 0$ one should apply the same criterion with respect to the magnetization $\boldsymbol{M}$ for small values of $|\boldsymbol{\psi}|$ near the phase transition line $T_{c2}(M)$;

$M = |\boldsymbol{M}|$. For this reason we should use the diagonal quadratic form [35] corresponding to the entire $\boldsymbol{\psi}^2$-part of the total free energy functional (1). The lowest energy term in this diagonal quadratic part contains a coefficient a of the form $a = (a_s - \gamma_0 M - \delta M^2)$ [35]. Now the equation $a(T) = 0$ defines the critical temperature of the Meissner phase and the equation $|a_s| = \mu_B M$ stands for $T_{c2}(M)$. It is readily seen that these two equations can be written in the same form, provided the parameter γ_0 in a is substituted by $\gamma_0' = (\gamma_0 - \mu_B)$. Thus the phase transition line corresponding to the vortex phase, described by the model (1) at zero external magnetic field and generated by the magnetization $\boldsymbol{M}$, can be obtained from the phase transition line corresponding to the uniform superconducting phase by an effective change of the value of the parameter γ_0. Both lines have the same shape and this is a particular property of the present model. The variation of the parameter γ_0 generates a family of lines.

Now we propose a possible way of theoretical treatment of the $T_{FS}(P)$ line of the FM-FS phase transition, shown in Fig. (1). This is a crucial point in our theory. The phase transition line of the uniform superconducting phase can be calculated within the thermodynamic analysis of the uniform phases, described by the free energy (1). This analysis is done in a simple variant of the free energy (1) in which the fields $\boldsymbol{\psi}$ and $\boldsymbol{M}$ do not depend on the spatial vector $\boldsymbol{x}$. The accomplishment of such analysis will give a formula for the phase transition line $T_{FS}(P)$ which corresponds a Meissner phase coexisting with the ferromagnetic order. The theoretical result for $T_{FS}(P)$ will contain a unspecified parameter γ_0. If the theoretical line $T_{FS}(P)$ is fitted to the experimental data for the FM-FS transition line corresponding to a particular compound, the two curves will coincide for some value of γ_0, irrespectively on the structure of the FS phase. If the FS phase contains a vortex superconductivity the fitting parameter $\gamma_{0(eff)}$ should be interpreted as γ_0' but if the FS phase contains Meissner superconductivity, $\gamma_{0(eff)}$ should be identified as γ_0. These arguments justify our approach to the investigation of the experimental data for the phase diagrams of intermetallic compounds with FM and FS phases. In the remainder of this paper, we shall investigate uniform phases.

3. Model considerations

In the previous section we have justified a thermodynamic analysis of the free energy (1) in terms of uniform order parameters. Neglecting the $\boldsymbol{x}$-dependence of $\boldsymbol{\psi}$ and $\boldsymbol{M}$, the free energy per unit volume, $F/V = f(\boldsymbol{\psi}, \boldsymbol{M})$ in zero external magnetic field ($\boldsymbol{H} = 0$), can be written in the form

$$f(\boldsymbol{\psi}, \boldsymbol{M}) = a_s|\boldsymbol{\psi}|^2 + \frac{b_s}{2}|\boldsymbol{\psi}|^4 + \frac{u_s}{2}|\boldsymbol{\psi}^2|^2 + \frac{v_s}{2}\sum_{j=1}^{3}|\psi_j|^4 + a_f\boldsymbol{M}^2 + \frac{b_f}{2}\boldsymbol{M}^4 + i\gamma_0\boldsymbol{M}\cdot(\boldsymbol{\psi}\times\boldsymbol{\psi}^*) + \delta_0\boldsymbol{M}^2|\boldsymbol{\psi}|^2. \quad (6)$$

Here we slightly modify the parameter a_f by choosing $a_f = \alpha_f[T^n - T_f^n(P)]$, where $n = 1$ gives the standard form of a_f, and $n = 2$ applies for SFT [30] and the Stoner-Wohlfarth model [36]. Previous studies [20] have shown that the anisotropy represented by the u_s and v_s terms in Eq. (6) slightly perturbs the size and shape of the stability domains of the phases, while similar effects can be achieved by varying the b_s factor in the $b_s|\boldsymbol{\psi}|^4$ term. For these reasons, in the present analysis we ignore the anisotropy terms, setting $u_s = v_s = 0$, and consider $b_s \equiv b > 0$ as an effective parameter. Then, without loss of generality, we are free to choose the magnetization vector to have the form $\boldsymbol{M} = (0, 0, M)$.

According to the microscopic theory of band magnetism and superconductivity the macroscopic material parameters in Eq. (6) depend in a quite complex way on the density of states at the Fermi level and related microscopic quantities [37]. That is why we can hardly use the microscopic characteristics of these complex metallic compounds in order to elucidate their thermodynamic properties, in particular, in outlining their phase diagrams in some details. However, some microscopic simple microscopic models reveal useful results, for example, the zero temperature Stoner-type model employed in Ref. [38].

We redefine for convenience the free energy (6) in a dimensionless form by $\tilde{f} = f/(b_f M_0^4)$, where $M_0 = [\alpha_f T_{f0}^n / b_f]^{1/2} > 0$ is the value of the magnetization M corresponding to the pure magnetic subsystem ($\boldsymbol{\psi} \equiv 0$) at $T = P = 0$ and $T_{f0} = T_f(0)$. The order parameters assume the scaling $m = M/M_0$ and $\boldsymbol{\varphi} = \boldsymbol{\psi}/[(b_f/b)^{1/4} M_0]$, and as a result, the free energy becomes

$$\tilde{f} = r\phi^2 + \frac{\phi^4}{2} + tm^2 + \frac{m^4}{2} + 2\gamma m\phi_1\phi_2 \sin\theta + \gamma_1 m^2\phi^2, \tag{7}$$

where $\phi_j = |\varphi_j|$, $\phi = |\boldsymbol{\varphi}|$, and $\theta = (\theta_2 - \theta_1)$ is the phase angle between the complex $\varphi_1 = \phi_1 e^{i\theta_1}$ and $\varphi_2 = \phi_2 e^{\theta_2}$. Note that the phase angle θ_3, corresponding to the third complex field component $\varphi_3 = \phi_3 e^{i\theta_3}$ does not enter explicitly in the free energy $\tilde{f}$, given by Eq. (7), which is a natural result of the continuous space degeneration. The dimensionless parameters t, r, γ and γ_1 in Eq. (7) are given by

$$t = \tilde{T}^n - \tilde{T}_f^n(P), \quad r = \kappa(\tilde{T} - \tilde{T}_s), \tag{8}$$

where $\kappa = \alpha_s b_f^{1/2}/\alpha_f b^{1/2} T_{f0}^{n-1}$, $\gamma = \gamma_0/[\alpha_f T_{f0}^n b]^{1/2}$, and $\gamma_1 = \delta_0/(b b_f)^{1/2}$. The reduced temperatures are $\tilde{T} = T/T_{f0}$, $\tilde{T}_f(P) = T_f(P)/T_{f0}$, and $\tilde{T}_s(P) = T_s(P)/T_{f0}$.

The analysis involves making simple assumptions for the P dependence of the t, r, γ, and γ_1 parameters in Eq. (7). Specifically, we assume that only T_f has a significant P dependence, described by

$$\tilde{T}_f(P) = (1 - \tilde{P})^{1/n}, \tag{9}$$

where $\tilde{P} = P/P_0$ and P_0 is a characteristic pressure deduced later. In $ZrZn_2$ and UGe_2 the P_0 values are very close to the critical pressure P_c at which both the ferromagnetic and superconducting orders vanish, but in other systems this is not necessarily the case. As we will discuss, the nonlinearity ($n = 2$) of $T_f(P)$ in $ZrZn_2$ and UGe_2 is relevant at relatively high P, at which the N-FM transition temperature $T_F(P)$ may not coincide with $T_f(P)$; $T_F(P)$ is the actual line of the N-FM phase transition, as shown in Fig. (1). The form (9) of the model function $\tilde{T}_f(P)$ is consistent with preceding experimental and theoretical investigations of the N-FM phase transition in $ZrZn_2$ and UGe_2 (see, e.g., Refs. [4, 24, 39]). Here we consider only non-negative values of the pressure P (for effects at $P < 0$, see, e.g., Ref. [44]).

The model function (9) is defined for $P \leq P_0$, in particular, for the case of $n > 1$, but we should have in mind that, in fact, the thermodynamic analysis of Eq. (7) includes the parameter t rather than $T_f(P)$. This parameter is given by

$$t(T, P) = \tilde{T}^n - 1 + \tilde{P}, \tag{10}$$

and is well defined for any $\tilde{P}$. This allows for the consideration of pressures $P > P_0$ within the free energy (7).

The model function $\tilde{T}_f(P)$ can be naturally generalized to $\tilde{T}_f(P) = (1 - \tilde{P}^{\beta})^{1/\alpha}$ but the present needs of interpretation of experimental data do not require such a complex consideration (hereafter we use Eq. (9) which corresponds to $\beta = 1$ and $\alpha = n$). Besides, other analytical forms of $\tilde{T}_f(\tilde{P})$ can also be tested in the free energy (7), in particular, expansion in powers of $\tilde{P}$, or, alternatively, in $(1 - \tilde{P})$ which satisfy the conditions $\tilde{T}_f(0) = 1$ and $\tilde{T}_f(1) = 0$. Note, that in URhGe the slope of $T_F(P) \sim T_f(P)$ is positive from $P = 0$ up to high pressures [8] and for this compound the form (9) of $\tilde{T}_f(P)$ is inconvenient. Here we apply the simplest variants of P-dependence, namely, Eqs. (9) and (10).

In more general terms, all material parameters (r, t, γ, ...) may depend on the pressure. We suppose that a suitable choice of the dependence of t on P is enough for describing the main thermodynamic properties and this supposition is supported by the final results, presented in the remainder of this paper. But in some particular investigations one may need to introduce a suitable pressure dependence of other parameters.

4. Stable phases

The simplified model (7) is capable of describing the main thermodynamic properties of spin-triplet ferromagnetic superconductors. For $r > 0$, i.e., $T > T_s$, there are three stable phases [20]: (i) the normal (N-) phase, given by $\phi = m = 0$ (stability conditions: $t \geq 0$, $r \geq 0$); (ii) the pure ferromagnetic phase (FM phase), given by $m = (-t)^{1/2} > 0$, $\phi = 0$, which exists for $t < 0$ and is stable provided $r \geq 0$ and $r \geq (\gamma_1 t + \gamma|t|^{1/2})$, and (iii) the already mentioned phase of coexistence of ferromagnetic order and superconductivity (FS phase), given by $\sin\theta = \mp 1$, $\phi_3 = 0$, $\phi_1 = \phi_2 = \phi/\sqrt{2}$, where

$$\phi^2 = \kappa(\tilde{T}_s - \tilde{T}) \pm \gamma m - \gamma_1 m^2 \geq 0. \tag{11}$$

The magnetization m satisfies the equation

$$c_3 m^3 \pm c_2 m^2 + c_1 m \pm c_0 = 0 \tag{12}$$

with coefficients $c_0 = \gamma\kappa(\tilde{T} - \tilde{T}_s)$,

$$c_1 = 2\left[\tilde{T}^n + \kappa\gamma_1(\tilde{T}_s - \tilde{T}) + \tilde{P} - 1 - \frac{\gamma^2}{2}\right], \tag{13}$$

$$c_2 = 3\gamma\gamma_1, \quad c_3 = 2(1 - \gamma_1^2). \tag{14}$$

The FS phase contains two thermodynamically equivalent phase domains that can be distinguished by the upper and lower signs ($\pm$) of some terms in Eqs. (11) and (12). The upper sign describes the domain (labelled bellow again by FS), where $m > 0$, $\sin\theta = -1$, whereas the lower sign describes the conjunct domain FS*, where $m < 0$ and $\sin\theta = 1$ (for details, see, Ref. [20]). Here we consider one of the two thermodynamically equivalent phase domains, namely, the domain FS, which is stable for $m > 0$ (FS* is stable for $m < 0$). This "one-domain approximation" correctly presents the main thermodynamic properties

N	$\tilde{T}_N$	t_N	$\tilde{P}_N(n)$
A	$\tilde{T}_s$	$\gamma^2/2$	$1-\tilde{T}_s^n+\gamma^2/2$
B	$\tilde{T}_s+\gamma^2(2+\gamma_1)/4\kappa(1+\gamma_1)^2$	$-\gamma^2/4(1+\gamma_1)^2$	$1-\tilde{T}_B^n-\gamma^2/4(1+\gamma_1)^2$
C	$\tilde{T}_s+\gamma^2/4\kappa(1+\gamma_1)$	0	$1-\tilde{T}_C^n$
max	$\tilde{T}_s+\gamma^2/4\kappa\gamma_1$	$-\gamma^2/4\gamma_1^2$	$1-\tilde{T}_m^n-\gamma^2/4\gamma_1^2$

Table 1. Theoretical results for the location [$(\tilde{T},\tilde{P})$ - reduced coordinates] of the tricritical points A $\equiv(\tilde{T}_A,\tilde{P}_A)$ and B $\equiv(\tilde{T}_B,\tilde{P}_B)$, the critical-end point C $\equiv(\tilde{T}_C,\tilde{P}_C)$, and the point of temperature maximum, max =$(\tilde{T}_m,\tilde{P}_m)$ on the curve $\tilde{T}_{FS}(\tilde{P})$ of the FM-FS phase transitions of first and second orders (for details, see Sec. 5). The first column shows $\tilde{T}_N\equiv\tilde{T}_{(A,B,C,m)}$. The second column stands for $t_N=t_{(A,B,C,m)}$. The reduced pressure values $\tilde{P}_{(A,B,C,m)}$ of points A, B, C, and max are denoted by $\tilde{P}_N(n)$: $n=1$ stands for the linear dependence $T_f(P)$, and $n=2$ stands for the nonlinear $T_f(P)$ and $t(T)$, corresponding to SFT.

described by the model (6), in particular, in the case of a lack of external symmetry breaking fields. The stability conditions for the FS phase domain given by Eqs.(11) and (12) are $\gamma M\geq 0$,

$$\kappa(\tilde{T}_s-\tilde{T})\pm\gamma m-2\gamma_1 m^2\geq 0, \tag{15}$$

and

$$3(1-\gamma_1^2)m^2+3\gamma\gamma_1 m+\tilde{T}^n-1+\tilde{P}+\kappa\gamma_1(\tilde{T}_s-\tilde{T})-\frac{\gamma^2}{2}\geq 0. \tag{16}$$

These results are valid whenever $T_f(P)>T_s(P)$, which excludes any pure superconducting phase ($\boldsymbol{\psi}\neq 0, m=0$) in accord with the available experimental data.

For $r<0$, and $t>0$ the models (6) and (7) exhibit a stable pure superconducting phase ($\phi_1=\phi_2=m=0$, $\phi_3^2=-r$) [20]. This phase may occur in the temperature domain $T_f(P)<T<T_s$. For systems, where $T_f(0)\gg T_s$, this is a domain of pressure in a very close vicinity of $P_0\sim P_c$, where $T_F(P)\sim T_f(P)$ decreases up to values lower than T_s. Of course, such a situation is described by the model (7) only if $T_s>0$. This case is interesting from the experimental point of view only when $T_s>0$ is enough above zero to enter in the scope of experimentally measurable temperatures. Up to date a pure superconducting phase has not been observed within the accuracy of experiments on the mentioned metallic compounds. For this reason, in the reminder of this paper we shall often assume that the critical temperature T_s of the generic superconducting phase transition is either non-positive ($T_s\leq 0$), or, has a small positive value which can be neglected in the analysis of the available experimental data.

The negative values of the critical temperature T_s of the generic superconducting phase transition are generally possible and produce a variety of phase diagram topologies (Sec. 5). Note, that the value of T_s depends on the strength of the interaction mediating the formation of the spin-triplet Cooper pairs of electrons. Therefore, for the sensitiveness of such electron couplings to the crystal lattice properties, the generic critical temperature T_s depends on the pressure. This is an effect which might be included in our theoretical scheme by introducing some convenient temperature dependence of T_s. To do this we need information either from experimental data or from a comprehensive microscopic theory.

Usually, $T_s\leq 0$ is interpreted as a lack of any superconductivity but here the same non-positive values of T_s are effectively enhanced to positive values by the interaction parameter γ which triggers the superconductivity up to superconducting phase-transition temperatures $T_{FS}(P)>0$. This is readily seen from Table 1, where we present the reduced critical temperatures on the FM-FS phase transition line $\tilde{T}_{FS}(\tilde{P})$, calculated from the present

theory, namely, $\tilde{T}_m$ – the maximum of the curve $T_{FS}(P)$ (if available, see Sec. 5), the temperatures $\tilde{T}_A$ and $\tilde{T}_B$, corresponding to the tricritical points A $\equiv (\tilde{T}_A, \tilde{P}_A)$ and B $\equiv (\tilde{T}_B, \tilde{P}_B)$, and the temperature $\tilde{T}_C$, corresponding to the critical-end point C $\equiv (\tilde{T}_C, \tilde{P}_C)$. The theoretical derivation of the dependence of the multicritical temperatures $\tilde{T}_A$, $\tilde{T}_B$ and $\tilde{T}_C$ on γ, γ_1, κ, and $\tilde{T}_s$, as well as the dependence of $\tilde{T}_m$ on the same model parameters is outlined in Sec. 5. All these temperatures as well as the whole phase transition line $T_{FS}(P)$ are considerably boosted above T_s owing to positive terms of order γ^2. If $\tilde{T}_s < 0$, the superconductivity appears, provided $\tilde{T}_m > 0$, i.e., when $\gamma^2/4\kappa\gamma_1 > |\tilde{T}_s|$ (see Table 1).

5. Temperature-pressure phase diagram

Although the structure of the FS phase is quite complicated, some of the results can be obtained in analytical form. A more detailed outline of the phase domains, for example, in $T - P$ phase diagram, can be done by using suitable values of the material parameters in the free energy (7): P_0, T_{f0}, T_s, κ, γ, and γ_1. Here we present some of the analytical results for the phase transition lines and the multi-critical points. Typical shapes of phase diagrams derived directly from Eq. (7) are given in Figs. 2–7. Figure 2 shows the phase diagram calculated from Eq. (7) for parameters, corresponding to the experimental data [13] for $ZrZn_2$. Figures 3 and 4 show the low-temperature and the high-pressure parts of the same phase diagram (see Sec. 7 for details). Figures 5–7 show the phase diagram calculated for the experimental data [2, 4] of UGe_2 (see Sec. 8). In $ZrZn_2$, UGe_2, as well as in UCoGe and UIr, critical pressure P_c exists, where both superconductivity and ferromagnetic orders vanish.

As in experiments, we find out from our calculation that in the vicinity of $P_0 \sim P_c$ the FM-FS phase transition is of fist order, denoted by the solid line BC in Figs. 3, 4, 6, and 7. At lower pressure the same phase transition is of second orderq shown by the dotted lines in the same figures. The second order phase transition line $\tilde{T}_{FS}(P)$ separating the FM and FS phases is given by the solution of the equation

$$\tilde{T}_{FS}(\tilde{P}) = \tilde{T}_s + \tilde{\gamma_1} t_{FS}(\tilde{P}) + \tilde{\gamma}[-t_{FS}(\tilde{P})]^{1/2}, \tag{17}$$

where $t_{FS}(\tilde{P}) = t(T_{FS}, \tilde{P}) \leq 0$, $\tilde{\gamma} = \gamma/\kappa$, $\tilde{\gamma}_1 = \gamma_1/\kappa$, and $0 < \tilde{P} < \tilde{P}_B$; P_B is the pressure corresponding to the multi-critical point B, where the line $T_{FS}(P)$ terminates, as clearly shown in Figs. 4 and 7). Note, that Eq. (17) strictly coincides with the stability condition for the FM phase with respect to appearance of FS phase [20].

Additional information for the shape of this phase transition line can be obtained by the derivative $\tilde{\rho} = \partial \tilde{T}_{FS}(\tilde{P})/\partial \tilde{P}$, namely,

$$\tilde{\rho} = \frac{\tilde{\rho}_s + \tilde{\gamma_1} - \tilde{\gamma}/2(-t_{FS})^{1/2}}{1 - n\tilde{T}_{FS}^{n-1}\left[\tilde{\gamma_1} - \tilde{\gamma}/2[(-t_{FS})^{1/2}\right]}, \tag{18}$$

where $\tilde{\rho}_s = \partial \tilde{T}_s(\tilde{P})/\partial \tilde{P}$. Note, that Eq. (18) is obtained from Eqs. (10) and (17).

The shape of the line $\tilde{T}_{FS}(P)$ can vary depending on the theory parameters (see, e.g., Figs.3 and 6). For certain ratios of $\tilde{\gamma}$, $\tilde{\gamma}_1$, and values of $\tilde{\rho}_s$, the curve $\tilde{T}_{FS}(\tilde{P})$ exhibits a maximum $\tilde{T}_m = \tilde{T}_{FS}(\tilde{P}_m)$, given by $\tilde{\rho}(\tilde{\rho}_s, T_m, P_m) = 0$. This maximum is clearly seen in Figs. 6 and 7. To locate the maximum we need to know $\tilde{\rho}_s$. We have already assumed T_s does not depend on P, as explained above, which from the physical point of view means that the function $T_s(P)$ is

flat enough to allow the approximation $\tilde{T}_s \approx 0$ without a substantial error in the results. From our choice of P-dependence of the free energy [Eq. (7)] parameters, it follow that $\tilde{\rho}_s = 0$.

Setting $\tilde{\rho}_s = \tilde{\rho} = 0$ in Eq. (18) we obtain

$$t(T_m, P_m) = -\frac{\tilde{\gamma}^2}{4\tilde{\gamma}_1^2}, \tag{19}$$

namely, the value $t_m(T,P) = t(T_m, P_m)$ at the maximum $T_m(P_m)$ of the curve $T_{FS}(P)$. Substituting t_m back in Eq. (17) we obtain T_m, and with its help we also obtain the pressure P_m, both given in Table 1, respectively.

We want to draw the attention to a particular feature of the present theory that the coordinates T_m and P_m of the maximum (point *max*) at the curve $T_{FS}(P)$ as well as the results from various calculations with the help of Eqs. (17) and (18) are expressed in terms of the reduced interaction parameters $\tilde{\gamma}$ and $\tilde{\gamma}_1$. Thus, using certain experimental data for T_m, P_m, as well as Eqs. (17) and (18) for T_{FS}, T_s, and the derivative ρ at particular values of the pressure P, $\tilde{\gamma}$ and $\tilde{\gamma}_1$ can be calculated without any additional information, for example, for the parameter κ. This property of the model (7) is quite useful in the practical work with the experimental data.

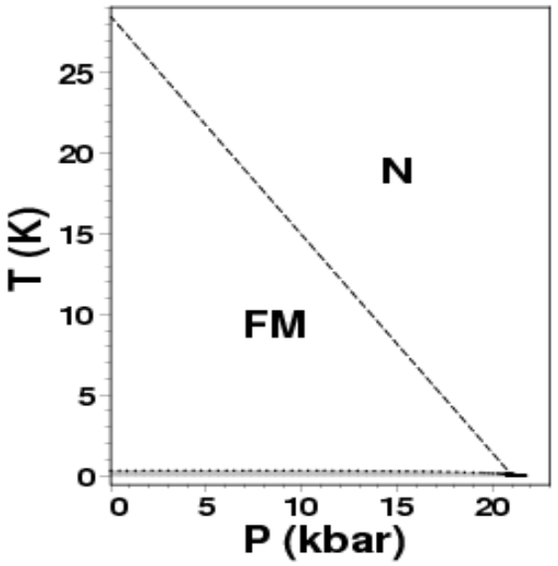

Figure 2. $T - P$ diagram of $ZrZn_2$ calculated for $T_s = 0$, $T_{f0} = 28.5$ K, $P_0 = 21$ kbar, $\kappa = 10$, $\tilde{\gamma} = 2\tilde{\gamma}_1 \approx 0.2$, and $n = 1$. The dotted line represents the FM-FS transition and the dashed line stands for the second order N-FM transition. The dotted line has a zero slope at $P = 0$. The low-temperature and high-pressure domains of the FS phase are seen more clearly in the following Figs. 3 and 4.

The conditions for existence of a maximum on the curve $T_{FS}(P)$ can be determined by requiring $\tilde{P}_m > 0$, and $\tilde{T}_m > 0$ and using the respective formulae for these quantities, shown in Table 1. This *max* always occurs in systems where $T_{FS}(0) \leq 0$ and the low-pressure part of the curve $T_{FS}(P)$ terminates at $T = 0$ for some non-negative critical pressure P_{0c} (see Sec. 6). But the *max* may occur also for some sets of material parameters, when $T_{FS}(0) > 0$ (see Fig. 3, where $P_m = 0$). All these shapes of the line $T_{FS}(P)$ are described by the model (7). Irrespectively of the particular shape, the curve $T_{FS}(P)$ given by Eq. (17) always terminates at the tricritical point (labeled B), with coordinates (P_B, T_B) (see, e.g., Figs. 4 and 7).

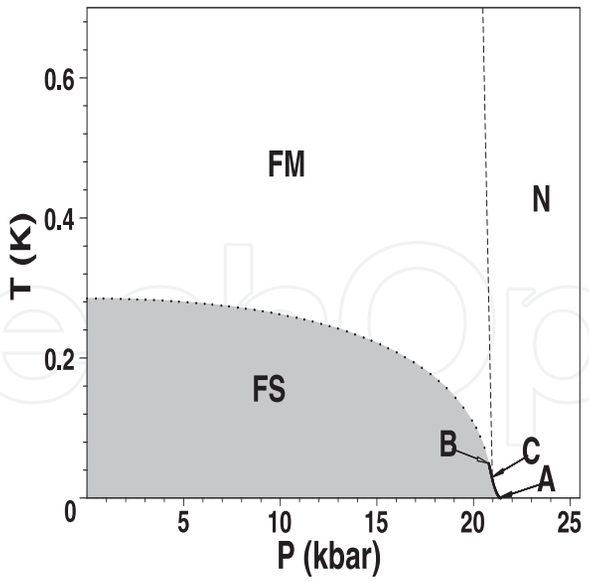

Figure 3. Details of Fig. 2 with expanded temperature scale. The points A, B, C are located in the high-pressure part ($P \sim P_c \sim 21$ kbar). The *max* point is at $P \approx 0$ kbar. The FS phase domain is shaded. The dotted line shows the second order FM-FS phase transition with $P_m \approx 0$. The solid straight line BC shows the fist-order FM-FS transition for $P > P_B$. The quite flat solid line AC shows the first order N-FS transition (the lines BC and AC are more clearly seen in Fig. 4. The dashed line stands for the second order N-FM transition.

At pressure $P > P_B$ the FM-FS phase transition is of first order up to the critical-end point C. For $P_B < P < P_C$ the FM-FS phase transition is given by the straight line BC (see, e.g., Figs. 4 and 7). The lines of all three phase transitions, N-FM, N-FS, and FM-FS, terminate at point C. For $P > P_C$ the FM-FS phase transition occurs on a rather flat smooth line of equilibrium transition of first order up to a second tricritical point A with $P_A \sim P_0$ and $T_A \sim 0$. Finally, the third transition line terminating at the point C describes the second order phase transition N-FM. The reduced temperatures $\tilde{T}_N$ and pressures $\tilde{P}_N$, N = (A, B, C, *max*) at the three multi-critical points (A, B, and C), and the maximum $T_m(P_m)$ are given in Table 1. Note that, for any set of material parameters, $T_A < T_C < T_B < T_m$ and $P_m < P_B < P_C < P_A$.

There are other types of phase diagrams, resulting from model (7). For negative values of the generic superconducting temperature T_s, several other topologies of the $T - P$ diagram can be outlined. The results for the multicritical points, presented in Table 1, shows that, when T_s lowers below $T = 0$, T_C also decreases, first to zero, and then to negative values. When $T_C = 0$ the direct N-FS phase transition of first order disappears and point C becomes a very special zero-temperature multicritical point. As seen from Table 1, this happens for $T_s = -\gamma^2 T_f(0)/4\kappa(1+\gamma_1)$. The further decrease of T_s causes point C to fall below the zero temperature and then the zero-temperature phase transition of first order near P_c splits into two zero-temperature phase transitions: a second order N-FM transition and a first order FM-FS transition, provided T_B still remains positive.

At lower T_s also point B falls below $T = 0$ and the FM-FS phase transition becomes entirely of second order. For very extreme negative values of T_s, a very large pressure interval below P_c may occur where the FM phase is stable up to $T = 0$. Then the line $T_{FS}(P)$ will exist only for relatively small pressure values $(P \ll P_c)$. This shape of the stability domain of the FS phase is also possible in real systems.

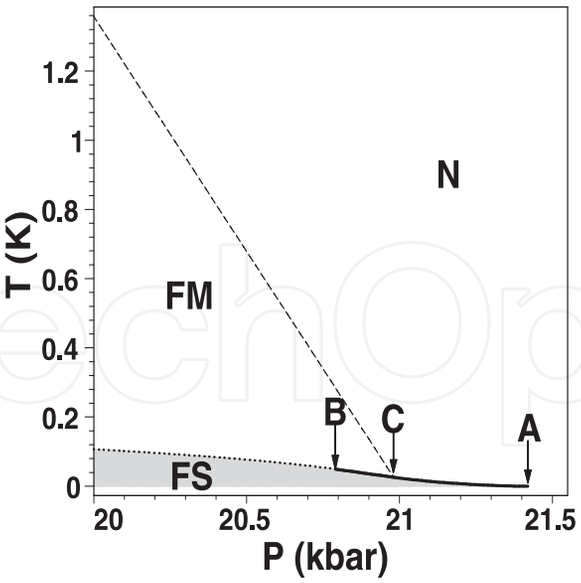

Figure 4. High-pressure part of the phase diagram of $ZrZn_2$, shown in Fig. 1. The thick solid lines AC and BC show the first-order transitions N-FS, and FM-FS, respectively. Other notations are explained in Figs. 2 and 3.

6. Quantum phase transitions

We have shown that the free energy (6) describes zero temperature phase transitions. Usually, the properties of these phase transitions essentially depend on the quantum fluctuations of the order parameters. For this reason the phase transitions at ultralow and zero temperature are called quantum phase transitions [31, 32]. The time-dependent quantum fluctuations (correlations) which describe the intrinsic quantum dynamics of spin-triplet ferromagnetic superconductors at ultralow temperatures are not included in our consideration but some basic properties of the quantum phase transitions can be outlines within the classical limit described by the free energy models (6) and (7). Let we briefly clarify this point.

The classical fluctuations are entirely included in the general GL functional (1)–(5) but the quantum fluctuations should be added in a further generalization of the theory. Generally, both classical (thermal) and quantum fluctuations are investigated by the method of the renormalization group (RG) [31], which is specially intended to treat the generalized action of system, where the order parameter fields ($\boldsymbol{\varphi}$ and $\boldsymbol{M}$) fluctuate in time t and space $\vec{x}$ [31, 32]. These effects, which are beyond the scope of the paper, lead either to a precise treatment of the narrow critical region in a very close vicinity of second order phase transition lines or to a fluctuation-driven change in the phase-transition order. But the thermal fluctuations and quantum correlation effects on the thermodynamics of a given system can be unambiguously estimated only after the results from counterpart simpler theory, where these phenomena are not present, are known and, hence, the distinction in the thermodynamic properties predicted by the respective variants of the theory can be established. Here we show that the basic low-temperature and ultralow-temperature properties of the spin-triplet ferromagnetic superconductors, as given by the preceding experiments, are derived from the model (6) without any account of fluctuation phenomena and quantum correlations. The latter might be of use in a more detailed consideration of the close vicinity of quantum critical points in the phase diagrams of ferromagnetic spin-triplet superconductors. Here we show that the theory predicts quantum critical phenomena only for quite particular physical conditions whereas

the low-temperature and zero-temperature phase transitions of first order are favored by both symmetry arguments and detailed thermodynamic analysis.

There is a number of experimental [9, 40] and theoretical [17, 41, 42] investigations of the problem for quantum phase transitions in unconventional ferromagnetic superconductors, including the mentioned intermetallic compounds. Some of them are based on different theoretical schemes and do not refer to the model (6). Others, for example, those in Ref. [41] reported results about the thermal and quantum fluctuations described by the model (6) before the comprehensive knowledge for the results from the basic treatment reported in the present investigation. In such cases one could not be sure about the correct interpretation of the results from the RG and the possibilities for their application to particular zero-temperature phase transitions. Here we present basic results for the zero-temperature phase transitions described by the model (6).

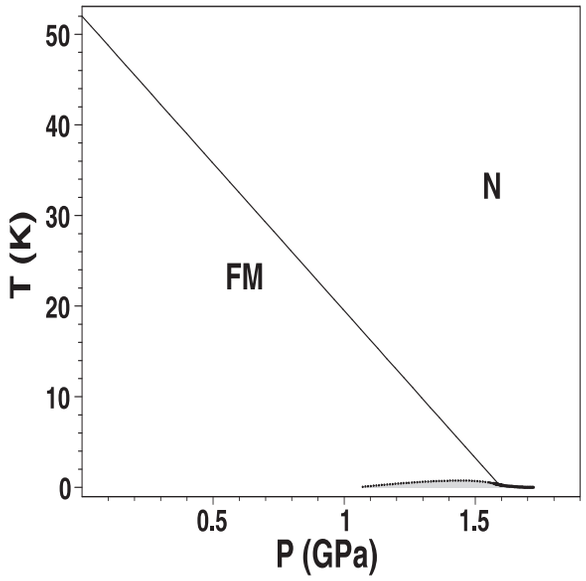

Figure 5. $T - P$ diagram of UGe_2 calculated taking $T_s = 0$, $T_{f0} = 52$ K, $P_0 = 1.6$ GPa, $\kappa = 4$, $\tilde{\gamma} = 0.0984$, $\tilde{\gamma_1} = 0.1678$, and $n = 1$. The dotted line represents the FM-FS transition and the dashed line stands for the N-FM transition. The low-temperature and high-pressure domains of the FS phase are seen more clearly in the following Figs. 6 and 7.

The RG investigation [41] has demonstrated up to two loop order of the theory that the thermal fluctuations of the order parameter fields rescale the model (6) in a way which corresponds to first order phase transitions in magnetically anisotropic systems. This result is important for the metallic compounds we consider here because in all of them magnetic anisotropy is present. The uniaxial magnetic anisotropy in $ZrZn_2$ is much weaker than in UGe_2 but cannot be neglected when fluctuation effects are accounted for. Owing to the particular symmetry of model (6), for the case of magnetic isotropy (Heisenberg symmetry), the RG study reveals an entirely different class of (classical) critical behavior. Besides, the different spatial dimensions of the superconducting and magnetic quantum fluctuations imply a lack of stable quantum critical behavior even when the system is completely magnetically isotropic. The pointed arguments and preceding results lead to the reliable conclusion that the phase transitions, which have already been proven to be first order in the lowest-order approximation, where thermal and quantum fluctuations are neglected, will not

undergo a fluctuation-driven change in the phase transition order from first to second. Such picture is described below, in Sec. 8, and it corresponds to the behavior of real compounds.

Our results definitely show that the quantum phase transition near P_c is of first order. This is valid for the whole N-FS phase transition below the critical-end point C, as well as the straight line BC. The simultaneous effect of thermal and quantum fluctuations do not change the order of the N-FS transition, and it is quite unlikely to suppose that thermal fluctuations of the superconductivity field $\boldsymbol{\psi}$ can ensure a fluctuation-driven change in the order of the FM-FS transition along the line BC. Usually, the fluctuations of $\boldsymbol{\psi}$ in low temperature superconductors are small and slightly influence the phase transition in a very narrow critical region in the vicinity of the phase-transition point. This effect is very weak and can hardly be observed in any experiment on low-temperature superconductors. Besides, the fluctuations of the magnetic induction $\boldsymbol{B}$ always tend to a fluctuation-induced first-order phase transition rather than to the opposite effect - the generation of magnetic fluctuations with infinite correlation length at the equilibrium phase-transition point and, hence, a second order phase transition [31, 43]. Thus we can quire reliably conclude that the first-order phase transitions at low-temperatures, represented by the lines BC and AC in vicinity of P_c do not change their order as a result of thermal and quantum fluctuation fluctuations.

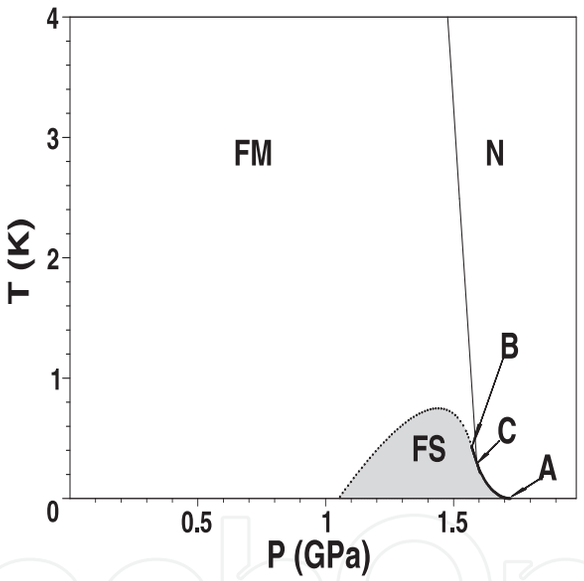

Figure 6. Low-temperature part of the $T - P$ phase diagram of UGe_2, shown in Fig. 5. The points A, B, C are located in the high-pressure part ($P \sim P_c \sim 1.6$ GPa). The FS phase domain is shaded. The thick solid lines AC and BC show the first-order transitions N-FS, and FM-FS, respectively. Other notations are explained in Figs. 2 and 3.

Quantum critical behavior for continuous phase transitions in spin-triplet ferromagnetic superconductors with magnetic anisotropy can therefore be observed at other zero-temperature transitions, which may occur in these systems far from the critical pressure P_c. This is possible when $T_{FS}(0) = 0$ and the $T_{FS}(P)$ curve terminates at $T = 0$ at one or two quantum (zero-temperature) critical points: $P_{0c} < P_m$ - "lower critical pressure", and $P'_{0c} > P_m$ – "upper critical pressure." In order to obtain these critical pressures one should solve Eq. (17) with respect to P, provided $T_{FS}(P) = 0$, $T_m > 0$ and $P_m > 0$, namely, when the continuous function $T_{FS}(P)$ exhibits a maximum. The critical pressure P'_{0c} is bounded

in the relatively narrow interval (P_m, P_B) and can appear for some special sets of material parameters (r, t, γ, γ_1). In particular, as our calculations show, P'_{0c} do not exists for $T_s \geq 0$.

7. Criteria for type I and type II spin-triplet ferromagnetic superconductors

The analytical calculation of the critical pressures P_{0c} and P'_{0c} for the general case of $T_s \neq 0$ leads to quite complex conditions for appearance of the second critical field P'_{0c}. The correct treatment of the case $T_s \neq 0$ can be performed within the entire two-domain picture for the phase FS (see, also, Ref. [20]). The complete study of this case is beyond our aims but here we will illustrate our arguments by investigation of the conditions, under which the critical pressure P_{oc} occurs in systems with $T_s \approx 0$. Moreover, we will present the general result for $P_{0c} \geq 0$ and $P'_{0c} \geq 0$ in systems where $T_s \neq 0$.

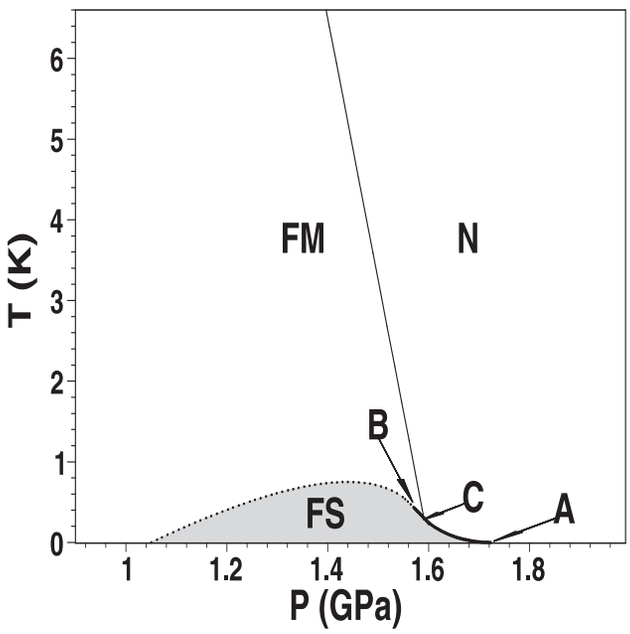

Figure 7. High-pressure part of the phase diagram of UGe_2, shown in Fig. 4. Notations are explained in Figs. 2, 3, 5, and 6.

Setting $T_{FS}(P_{0c}) = 0$ in Eq. (17) we obtain the following quadratic equation,

$$\tilde{\gamma}_1 m_{0c}^2 - \tilde{\gamma} m_{0c} - \tilde{T}_s = 0, \tag{20}$$

for the reduced magnetization,

$$m_{0c} = [-t(0, \tilde{P}_{oc})]^{1/2} = (1 - \tilde{P}_{0c})^{1/2} \tag{21}$$

and, hence, for $\tilde{P}_{0c}$. For $T_s \neq 0$, Eqs. (20) and (21) have two solutions with respect to $\tilde{P}_{0c}$. For some sets of material parameters these solutions satisfy the physical requirements for P_{0c} and P'_{0c} and can be identified with the critical pressures. The conditions for existence of P_{0c} and P'_{0c} can be obtained either by analytical calculations or by numerical analysis for particular values of the material parameters.

For $T_s = 0$, the trivial solution $\tilde{P}_{0c} = 1$ corresponds to $P_{0c} = P_0 > P_B$ and, hence, does not satisfy the physical requirements. The second solution,

$$\tilde{P}_{0c} = 1 - \frac{\tilde{\gamma}^2}{\tilde{\gamma}_1^2} \tag{22}$$

is positive for

$$\frac{\gamma_1}{\gamma} \geq 1 \tag{23}$$

and, as shown below, it gives the location of the quantum critical point ($T = 0, P_{0c} < P_m$). At this quantum critical point, the equilibrium magnetization m_{0c} is given by $m_{0c} = \gamma/\gamma_1$ and is twice bigger that the magnetization $m_m = \gamma/2\gamma_1$ ([20]) at the maximum of the curve $T_{FS}(P)$.

To complete the analysis we must show that the solution (22) satisfies the condition $P_{0c} < \tilde{P}_m$. By taking $\tilde{P}_m$ from Table 1, we can show that solution (22) satisfies the condition $P_{0c} < \tilde{P}_m$ for $n = 1$, if

$$\gamma_1 < 3\kappa, \tag{24}$$

and for $n = 2$ (SFT case), when

$$\gamma < 2\sqrt{3}\kappa. \tag{25}$$

Finally, we determine the conditions under which the maximum T_m of the curve $T_{FS}(P)$ occurs at non-negative pressures. For $n = 1$, we obtain that $P_m \geq 0$ for $n = 1$, if

$$\frac{\gamma_1}{\gamma} \geq \frac{1}{2}\left(1 + \frac{\gamma_1}{\kappa}\right)^{1/2}, \tag{26}$$

whereas for $n = 2$, the condition is

$$\frac{\gamma_1}{\gamma} \geq \frac{1}{2}\left(1 + \frac{\gamma^2}{4\kappa^2}\right)^{1/2}. \tag{27}$$

Obviously, the conditions (23)-(27) are compatible with one another. The condition (26) is weaker than the condition Eq. (23), provided the inequality (24) is satisfied. The same is valid for the condition (27) if the inequality (25) is valid. In Sec. 8 we will show that these theoretical predictions are confirmed by the experimental data.

Doing in the same way the analysis of Eq. (17), some results may easily obtained for $T_s \neq 0$. In this more general case the Eq. (17) has two nontrivial solutions, which yield two possible values of the critical pressure

$$\tilde{P}_{0c(\pm)} = 1 - \frac{\gamma^2}{4\gamma_1^2}\left[1 \pm \left(1 + \frac{4\tilde{T}_s\kappa\gamma_1}{\gamma^2}\right)^{1/2}\right]^2. \tag{28}$$

The relation $\tilde{P}_{0c(-)} \geq \tilde{P}_{0c(+)}$ is always true. Therefore, to have both $\tilde{P}_{0c(\pm)} \geq 0$, it is enough to require $\tilde{P}_{0c(+)} \geq 0$. Having in mind that for the phase diagram shape, we study $\tilde{T}_m > 0$, and

according to the result for $\tilde{T}_m$ in Table 1, this leads to the inequality $\tilde{T}_s > -\gamma^2/4\kappa\gamma_1$. So, we obtain that $\tilde{P}_{0c(+)} \geq 0$ will exist, if

$$\frac{\gamma_1}{\gamma} \geq 1 + \frac{\kappa\tilde{T}_s}{\gamma}, \tag{29}$$

which generalizes the condition (23).

Now we can identify the pressure $P_{0c(+)}$ with the lower critical pressure P_{0c}, and $P_{0c(-)}$ with the upper critical pressure P'_{0c}. Therefore, for wide variations in the parameters, theory (6) describes a quantum critical point P_{oc}, that exists, provided the condition (29) is satisfied. The quantum critical point $(T = 0, P_{0c})$ exists in UGe_2 and, perhaps, in other p-wave ferromagnetic superconductors, for example, in UIr.

Our results predict the appearance of second critical pressure – the upper critical pressure P'_{oc} that exists under more restricted conditions and, hence, can be observed in more particular systems, where $T_s < 0$. As mentioned in Sec. 5, for very extreme negative values of T_s, when $T_B < 0$, the upper critical pressure $P'_{0c} > 0$ occurs, whereas the lower critical pressure $P_{0c} > 0$ does not appear. Bue especially this situation should be investigated in a different way, namely, one should keep $T_{FS}(0)$ different from zero in Eq. (17), and consider a form of the FS phase domain in which the curve $T_{FS}(P)$ terminates at $T = 0$ for $P'_{0c} > 0$, irrespective of whether the maximum T_m exists or not. In such geometry of the FS phase domain, the maximum $T(P_m)$ may exist only in quite unusual cases, if it exists at all.

Using criteria like (23) in Sec. 8.4 we classify these superconductors in two types: (i) type I, when the condition (23) is satisfied, and (ii) type II, when the same condition does not hold. As we show in Sec. 8.2, 8.3 and 8.4, the condition (23) is satisfied by UGe_2 but the same condition fails for $ZrZn_2$. For this reason the phase diagrams of UGe_2 and $ZrZn_2$ exhibit qualitatively different shapes of the curves $T_FS(P)$. For UGe_2 the line $T_FS(P)$ has a maximum at some pressure $P > 0$, whereas the line $T_FS(P)$, corresponding to $ZrZn_2$, does not exhibit such maximum (see also Sec. 8).

The quantum and thermal fluctuation phenomena in the vicinities of the two critical pressures P_{0c} and P'_{0c} need a nonstandard RG treatment because they are related with the fluctuation behavior of the superconducting field $\boldsymbol{\psi}$ far below the ferromagnetic phase transitions, where the magnetization $\boldsymbol{M}$ does not undergo significant fluctuations and can be considered uniform. The presence of uniform magnetization produces couplings of $\boldsymbol{M}$ and $\boldsymbol{\psi}$ which are not present in previous RG studies and need a special analysis.

8. Application to metallic compounds

8.1. Theoretical outline of the phase diagram

In order to apply the above displayed theoretical calculations, following from free energy (7), for the outline of $T - P$ diagram of any material, we need information about the values of P_0, T_{f0}, T_s, κ γ, and γ_1. The temperature T_{f0} can be obtained directly from the experimental phase diagrams. The pressure P_0 is either identical or very close to the critical pressure P_c, for which the N-FM phase transition line terminates at $T \sim 0$. The temperature T_s of the generic superconducting transition is not available from the experiments because, as mentioned above, pure superconducting phase not coexisting with ferromagnetism has not

been observed. This can be considered as an indication that T_s is very small and does not produce a measurable effect. So the generic superconducting temperature will be estimated on the basis of the following arguments. For $T_f(P) > T_s$ we must have $T_s(P) = 0$ at $P \geq P_c$, where $T_f(P) \leq 0$, and for $0 \leq P \leq P_0$, $T_s < T_C$. Therefore for materials where T_C is too small to be observed experimentally, T_s can be ignored.

As far as the shape of FM-FS transition line is well described by Eq. (17), we will make use of additional data from available experimental phase diagrams for ferroelectric superconductors. For example, in $ZrZn_2$ these are the observed values of $T_{FS}(0)$ and the slope $\rho_0 \equiv [\partial T_{FS}(P)/\partial P]_0 = (T_{f0}/P_0)\tilde{\rho}_0$ at $P = 0$; see Eq. (17). For UGe_2, where a maximum ($\tilde{T}_m$) is observed on the phase-transition line, we can use the experimental values of T_m, P_m, and P_{0c}. The interaction parameters $\tilde{\gamma}$ and $\tilde{\gamma}_1$ are derived using Eq. (17), and the expressions for $\tilde{T}_m$, $\tilde{P}_m$, and $\tilde{\rho}_0$, see Table 1. The parameter κ is chosen by fitting the expression for the critical-end point T_C.

8.2. $ZrZn_2$

Experiments for $ZrZn_2$ [13] gives the following values: $T_{f0} = 28.5$ K, $T_{FS}(0) = 0.29$ K, $P_0 \sim P_c = 21$ kbar. The curve $T_F(P) \sim T_f(P)$ is almost a straight line, which directly indicates that $n = 1$ is adequate in this case for the description of the P-dependence. The slope for $T_{FS}(P)$ at $P = 0$ is estimated from the condition that its magnitude should not exceed $T_{f0}/P_c \approx 0.014$ as we have assumed that is straight one, so as a result we have $-0.014 < \rho \leq 0$. This ignores the presence of a maximum. The available experimental data for $ZrZn_2$ do not give clear indication whether a maximum at (T_m, P_m) exists. If such a maximum were at $P = 0$ we would have $\rho_0 = 0$, whereas a maximum with $T_m \sim T_{FS}(0)$ and $P_m \ll P_0$ provides us with an estimated range $0 \leq \rho_0 < 0.005$. The choice $\rho_0 = 0$ gives $\tilde{\gamma} \approx 0.02$ and $\tilde{\gamma}_1 \approx 0.01$, but similar values hold for any $|\rho_0| \leq 0.003$. The multicritical points A and C cannot be distinguished experimentally. Since the experimental accuracy [13] is less than ~ 25 mK in the high-P domain ($P \sim 20 - 21$ kbar), we suppose that $T_C \sim 10$ mK, which corresponds to $\kappa \sim 10$. We employed these parameters to calculate the $T - P$ diagram using $\rho_0 = 0$ and 0.003. The differences obtained in these two cases are negligible, with both phase diagrams being in excellent agreement with experiment.

Phase diagram of $ZrZn_2$ calculated directly from the free energy (7) for $n = 1$, the above mentioned values of T_s, P_0, T_{f0}, κ, and values of $\tilde{\gamma} \approx 0.2$ and $\tilde{\gamma}_1 \approx 0.1$ which ensure $\rho_0 \approx 0$ is shown in Fig. 2. Note, that the experimental phase diagram [13] of $ZrZn_2$ looks almost exactly as the diagram in Fig. 2, which has been calculated directly from the model (7) without any approximations and simplifying assumptions. The phase diagram in Fig. 2 has the following coordinates of characteristic points: $P_A \sim P_c = 21.42$ kbar, $P_B = 20.79$ kbar, $P_C = 20.98$ kbar, $T_A = T_F(P_c) = T_{FS}(P_c) = 0$ K, $T_B = 0.0495$ K, $T_C = 0.0259$ K, and $T_{FS}(0) = 0.285$ K.

The low-T region is seen in more detail in Fig. 3, where the A, B, C points are shown and the order of the FM-FS phase transition changes from second to first order around the critical end-point C. The $T_{FS}(P)$ curve, shown by the dotted line in Fig. 3, has a maximum $T_m = 0.290$ K at $P = 0.18$ kbar, which is slightly above $T_{FS}(0) = 0.285$ K. The straight solid line BC in Fig. 3 shows the first order FM-FS phase transition which occurs for $P_B < P < P_C$. The solid AC line shows the first order N-FS phase transition and the dashed line stands for the N-FM phase transition of second order.

Although the expanded temperature scale in Fig. 3, the difference $[T_m - T_{FS}(0)] = 5$ mK is hard to see. To locate the point *max* exactly at $P = 0$ one must work with values of $\tilde{\gamma}$ and $\tilde{\gamma}_1$ of accuracy up to 10^{-4}. So, the location of the *max* for parameters corresponding to $ZrZn_2$ is very sensitive to small variations of $\tilde{\gamma}$ and $\tilde{\gamma}_1$ around the values 0.2 and 0.1, respectively. Our initial idea was to present a diagram with $T_m = T_{FS}(0) = 0.29$ K and $\rho_0 = 0$, namely, *max* exactly located at $P = 0$, but the final phase diagram slightly departs from this picture because of the mentioned sensitivity of the result on the values of the interaction parameters γ and γ_1. The theoretical phase diagram of $ZrZn_2$ can be deduced in the same way for $\rho_0 = 0.003$ and this yields $T_m = 0.301$ K at $P_m = 6.915$ kbar for initial values of $\tilde{\gamma}$ and $\tilde{\gamma}_1$ which differs from $\tilde{\gamma} = 2\tilde{\gamma}_1 = 0.2$ only by numbers of order $10^{-3} - 10^{-4}$ [18]. This result confirms the mentioned sensitivity of the location of the maximum T_m towards slight variations of the material parameters. Experimental investigations of this low-temperature/low-pressure region with higher accuracy may help in locating this maximum with better precision.

Fig. 4 shows the high-pressure part of the same phase diagram in more details. In this figure the first order phase transitions (solid lines BC and AC) are clearly seen. In fact the line AC is quite flat but not straight as the line BC. The quite interesting topology of the phase diagram of $ZrZn_2$ in the high-pressure domain ($P_B < P < P_A$) is not seen in the experimental phase diagram [13] because of the restricted accuracy of the experiment in this range of temperatures and pressures.

These results account well for the main features of the experimental behavior [13], including the claimed change in the order of the FM-FS phase transition at relatively high P. Within the present model the N-FM transition is of second order up to $P_C \sim P_c$. Moreover, if the experiments are reliable in their indication of a first order N-FM transition at much lower P values, the theory can accommodate this by a change of sign of b_f, leading to a new tricritical point located at a distinct $P_{tr} < P_C$ on the N-FM transition line. Since $T_C > 0$ a direct N-FS phase transition of first order is predicted in accord with conclusions from de Haas–van Alphen experiments [44] and some theoretical studies [40]. Such a transition may not occur in other cases where $T_C = 0$. In SFT ($n = 2$) the diagram topology remains the same but points B and C are slightly shifted to higher P (typically by about $0.01 - -0.001$ kbar).

8.3. UGe_2

The experimental data for UGe_2 indicate $T_{f0} = 52$ K, $P_c = 1.6$ GPa ($\equiv 16$ kbar), $T_m = 0.75$ K, $P_m \approx 1.15$ GPa, and $P_{0c} \approx 1.05$ GPa [2–5]. Using again the variant $n = 1$ for $T_f(P)$ and the above values for T_m and P_{0c} we obtain $\tilde{\gamma} \approx 0.0984$ and $\tilde{\gamma}_1 \approx 0.1678$. The temperature $T_C \sim 0.1$ K corresponds to $\kappa \sim 4$.

Using these initial parameters, together with $T_s = 0$, leads to the $T - P$ diagram of UGE_2 shown in Fig. 5. We obtain $T_A = 0$ K, $P_A = 1.723$ GPa, $T_B = 0.481$ K, $P_B = 1.563$ GPa, $T_C = 0.301$ K, and $P_C = 1.591$ GPa. Figs. 6 and 7 show the low-temperature and the high-pressure parts of this phase diagram, respectively. There is agreement with the main experimental findings, although P_m corresponding to the maximum (found at ~ 1.44 GPa in Fig. 5) is about 0.3 GPa higher than suggested experimentally [4, 5]. If the experimental plots are accurate in this respect, this difference may be attributable to the so-called (T_x) meta-magnetic phase transition in UGe_2, which is related to an abrupt change of the magnetization in the vicinity of P_m. Thus, one may suppose that the meta-magnetic effects, which are outside the scope of our current model, significantly affect the shape of the $T_{FS}(P)$ curve by lowering P_m (along

with P_B and P_C). It is possible to achieve a lower P_m value (while leaving T_m unchanged), but this has the undesirable effect of modifying P_{c0} to a value that disagrees with experiment. In SFT ($n = 2$) the multi-critical points are located at slightly higher P (by about 0.01 GPa), as for $ZrZn_2$. Therefore, the results from the SFT theory are slightly worse than the results produced by the usual linear approximation ($n = 1$) for the parameter t.

8.4. Two types of ferromagnetic superconductors with spin-triplet electron pairing

The estimates for UGe_2 imply $\gamma_1\kappa \approx 1.9$, so the condition for $T_{FS}(P)$ to have a maximum found from Eq. (17) is satisfied. As we discussed for $ZrZn_2$, the location of this maximum can be hard to fix accurately in experiments. However, P_{c0} can be more easily distinguished, as in the UGe_2 case. Then we have a well-established quantum (zero-temperature) phase transition of second order, i.e., a quantum critical point at some critical pressure $P_{0c} \geq 0$. As shown in Sec. 6, under special conditions the quantum critical points could be two: at the lower critical pressure $P_{0c} < P_m$ and the upper critical pressure $P'_{0c} < P_m$. This type of behavior in systems with $T_s = 0$ (as UGe_2) occurs when the criterion (23) is satisfied. Such systems (which we label as U-type) are essentially different from those such as $ZrZn_2$ where $\gamma_1 < \gamma$ and hence $T_{FS}(0) > 0$. In this latter case (Zr-type compounds) a maximum $T_m > 0$ may sometimes occur, as discussed earlier. We note that the ratio γ/γ_1 reflects a balance effect between the two $\boldsymbol{\psi}$-$\boldsymbol{M}$ interactions. When the trigger interaction (typified by γ) prevails, the Zr-type behavior is found where superconductivity exists at $P = 0$. The same ratio can be expressed as $\gamma_0/\delta_0 M_0$, which emphasizes that the ground state value of the magnetization at $P = 0$ is also relevant. Alternatively, one may refer to these two basic types of spin-triplet ferromagnetic superconductors as "type I" (for example, for the "Zr-type compounds), and "type II" – for the U-type compounds.

As we see from this classification, the two types of spin-triplet ferromagnetic superconductors have quite different phase diagram topologies although some fragments have common features. The same classification can include systems with $T_s \neq 0$ but in this case one should use the more general criterion (29).

8.5. Other compounds

In URhGe, $T_f(0) \sim 9.5$ K and $T_{FS}(0) = 0.25$ K and, therefore, as in $ZrZn_2$, here the spin-triplet superconductivity appears at ambient pressure deeply in the ferromagnetic phase domain [6–8]. Although some similar structural and magnetic features are found in UGe_2 the results in Ref. [8] of measurements under high pressure show that, unlike the behavior of $ZrZn_2$ and UGe_2, the ferromagnetic phase transition temperature $T_F(P) \sim T_f(P)$ has a slow linear increase up to 140 kbar without any experimental indications that the N-FM transition line may change its behavior at higher pressures and show a negative slope in direction of low temperature up to a quantum critical point $T_F = 0$ at some critical pressure P_c. Such a behavior of the generic ferromagnetic phase transition temperature cannot be explained by our initial assumption for the function $T_f(P)$ which was intended to explain phase diagrams where the ferromagnetic order is depressed by the pressure and vanishes at $T = 0$ at some critical pressure P_c. The $T_{FS}(P)$ line of URhGe shows a clear monotonic negative slope to $T = 0$ at pressures above 15 kbar and the extrapolation [8] of the experimental curve $T_{FS}(P)$ tends a quantum critical point $T_{FS}(P'_{oc}) = 0$ at $P_{0c} \sim 25 - 30$ kbar. Within the

framework of the phenomenological theory (6, this $T-P$ phase diagram can be explained after a modification on the $T_f(P)$-dependence is made, and by introducing a convenient nontrivial pressure dependence of the interaction parameter γ. Such modifications of the present theory are possible and follow from important physical requirements related with the behavior of the f-band electrons in URhGe. Unlike UGe_2, where the pressure increases the hybridization of the $5f$ electrons with band states lading to a suppression of the spontaneous magnetic moment M, in URhGe this effects is followed by a stronger effect of enhancement of the exchange coupling due to the same hybridization, and this effect leads to the slow but stable linear increase in the function $T_F(P)$[8]. These effects should be taken into account in the modeling the pressure dependence of the parameters of the theory (7) when applied to URhGe.

Another ambient pressure FS phase has been observed in experiments with UCoGe [9]. Here the experimentally derived slopes of the functions $T_F(P)$ and $T_{FS}(P)$ at relatively small pressures are opposite compared to those for URhGe and, hence, the $T-P$ phase diagram of this compound can be treated within the present theoretical scheme without substantial modifications.

Like in UGe_2, the FS phase in UIr [12] is embedded in the high-pressure/low-temperature part of the ferromagnetic phase domain near the critical pressure P_c which means that UIr is certainly a U-type compound. In UGe_2 there is one metamagnetic phase transition between two ferromagnetic phases (FM1 and FM2), in UIr there are three ferromagnetic phases and the FS phase is located in the low-T/high-P domain of the third of them - the phase FM3. There are two metamagnetic-like phase transitions: FM1-FM2 transition which is followed by a drastic decrease of the spontaneous magnetization when the the lower-pressure phase FM1 transforms to FM2, and a peak of the ac susceptibility but lack of observable jump of the magnetization at the second (higher pressure) “metamagnetic" phase transition from FM2 to FM3. Unlike the picture for UGe_2, in UIr both transitions, FM1-FM2 and FM2-FM3 are far from the maximum $T_m(P_m)$ so in this case one can hardly speculate that the *max* is produced by the nearby jump of magnetization. UIr seems to be a U-type spin-triplet ferromagnetic superconductor.

9. Final remarks

Finally, even in its simplified form, this theory has been shown to be capable of accounting for a wide variety of experimental behavior. A natural extension to the theory is to add a $\boldsymbol{M}^6$ term which provides a formalism to investigate possible metamagnetic phase transitions [45] and extend some first order phase transition lines. Another modification of this theory, with regard to applications to other compounds, is to include a P dependence for some of the other GL parameters. The fluctuation and quantum correlation effects can be considered by the respective field-theoretical action of the system, where the order parameters $\boldsymbol{\psi}$ and $\boldsymbol{M}$ are not uniform but rather space and time dependent. The vortex (spatially non-uniform) phase due to the spontaneous magnetization $\boldsymbol{M}$ is another phenomenon which can be investigated by a generalization of the theory by considering nonuniform order parameter fields $\boldsymbol{\psi}$ and $\boldsymbol{M}$ (see, e.g., Ref. [28]). Note that such theoretical treatments are quite complex and require a number of approximations. As already noted in this paper the magnetic fluctuations stimulate first order phase transitions for both finite and zero phase-transition temperatures.

Author details

Dimo I. Uzunov
Collective Phenomena Laboratory, G. Nadjakov Institute of Solid State Physics, Bulgarian Academy of Sciences, BG-1784 Sofia, Bulgaria.
Pacs: 74.20.De, 74.25.Dw, 64.70.Tg

10. References

[1] D. Vollhardt and P. Wölfle, it The Superfluid Phases of Helium 3 (Taylor & Francis, London, 1990); D. I. Uzunov, in: *Advances in Theoretical Physics*, edited by E. Caianiello (World Scientific, Singapore, 1990), p. 96; M. Sigrist and K. Ueda, Rev. Mod. Phys. 63, 239 (1991).
[2] S. S. Saxena, P. Agarwal, K. Ahilan, F. M. Grosche, R. K. W. Haselwimmer, M.J. Steiner, E. Pugh, I. R. Walker, S.R. Julian, P. Monthoux, G. G. Lonzarich, A. Huxley. I. Sheikin, D. Braithwaite, and J. Flouquet, Nature 406, 587 (2000).
[3] A. Huxley, I. Sheikin, E. Ressouche, N. Kernavanois, D. Braithwaite, R. Calemczuk, and J. Flouquet, Phys. Rev. B63, 144519 (2001).
[4] N. Tateiwa, T. C. Kobayashi, K. Hanazono, A. Amaya, Y. Haga. R. Settai, and Y. Onuki, J. Phys. Condensed Matter 13, L17 (2001).
[5] A. Harada, S. Kawasaki, H. Mukuda, Y. Kitaoka, Y. Haga, E. Yamamoto, Y. Onuki, K. M. Itoh, E. E. Haller, and H. harima, Phys. Rev. B 75, 140502 (2007).
[6] D. Aoki, A. Huxley, E. Ressouche, D. Braithwaite, J. Flouquet, J-P.. Brison, E. Lhotel, and C. Paulsen, Nature 413, 613 (2001).
[7] F. Hardy, A. Huxley, Phys. Rev. Lett. 94, 247006 (2005).
[8] F. Hardy, A. Huxley, J. Flouquet, B. Salce, G. Knebel, D. Braithwate, D. Aoki, M. Uhlarz, and C. Pfleiderer, Physica B 359-361 1111 (2005).
[9] N. T. Huy, A. Gasparini, D. E. de Nijs, Y. Huang, J. C. P. Klaasse, T. Gortenmulder, A. de Visser, A. Hamann, T. Görlach, and H. v. Löhneysen, Phys. Rev. Lett. 99, 067006 (2007).
[10] N. T. Huy, D. E. de Nijs, Y. K. Huang, and A. de Visser, Phys. Rev. Lett. 100, 077001 (2008).
[11] T. Akazawa, H. Hidaka, H. Kotegawa, T. C. Kobayashi, T. Fujiwara, E. Yamamoto, Y. Haga, R. Settai, and Y. Onuki, Physica B 359-361, 1138 (2005).
[12] T. C. Kobayashi,S. Fukushima, H. Hidaka, H. Kotegawa, T. Akazawa, E. Yamamoto, Y. Haga, R. Settai, and Y. Onuki, Physica B 378-361, 378 (2006).
[13] C. Pfleiderer, M. Uhlatz, S. M. Hayden, R. Vollmer, H. v. Löhneysen, N. R. Berhoeft, and G. G. Lonzarich, Nature 412, 58 (2001).
[14] E. A. Yelland, S. J. C. Yates, O. Taylor, A. Griffiths, S. M. Hayden, and A. Carrington, Phys. Rev. B 72, 184436 (2005).
[15] E. A. Yelland, S. M. Hayden, S. J. C. Yates, C. Pfleiderer, M. Uhlarz, R. Vollmer, H. v Löhneysen, N. R. Bernhoeft, R. P. Smith, S. S. Saxena, and N. Kimura, Phys. Rev. B72, 214523 (2005).
[16] C. J. Bolesh and T. Giamarchi, Phys. Rev. Lett. 71, 024517 (2005); R. D. Duncan, C. Vaccarella, and C. A. S. de Melo, Phys. Rev. B 64, 172503 (2001).
[17] A. H. Nevidomskyy, Phys. Rev. Lett. 94, 097003 (2005).
[18] M. G. Cottam, D. V. Shopova and D. I. Uzunov, Phys. Lett. A 373, 152 (2008).

[19] D. V. Shopova and D. I. Uzunov, Phys. Rev. B 79, 064501 (2009).
[20] D. V. Shopova and D. I. Uzunov, Phys. Rev. 72, 024531 (2005); Phys. Lett. A 313, 139 (2003).
[21] D. V. Shopova and D. I. Uzunov, in: *Progress in Ferromagnetism Research*, ed. by V. N. Murray (Nova Science Publishers, New York, 2006), p. 223; D. V. Shopova and D. I. Uzunov, J. Phys. Studies , 4, 426 (2003) 426; D. V. Shopova and D. I. Uzunov, Compt. Rend Acad. Bulg. Sci. 56, 35 (2003) 35; D. V. Shopova, T. E. Tsvetkov, and D. I. Uzunov, Cond. Matter Phys. 8, 181 (2005) 181; D. V. Shopova, and D. I. Uzunov, Bulg. J. of Phys. 32, 81 (2005).
[22] E. K. Dahl and A. Sudbø, Phys. Rev. B 75, 1444504 (2007).
[23] K. Machida and T. Ohmi, Phys. Rev. Lett. 86, 850 (2001).
[24] M. B. Walker and K. V. Samokhin, Phys. Rev. Lett. 88, 207001 (2002); K. V. Samokhin and M. B. Walker, Phys. Rev. B 66, 024512 (2002); Phys. Rev. B 66, 174501 (2002).
[25] J. Linder, A. Sudbø, Phys. Rev. B 76, 054511 (2007); J. Linder, I. B. Sperstad, A. H. Nevidomskyy, M. Cuoco, and A. Sodbø, Phys. Rev. 77, 184511 (2008); J. Linder, T. Yokoyama, and A. Sudbø, Phys. Rev. B 78, 064520 (2008); J. Linder, A. H. Nevidomskyy, A. Sudbø, Phys. Rev. B 78, 172502 (2008).
[26] R. A. Cowley, Adv. Phys. 29, 1 (1980); J-C. Tolédano and P. Tolédano, *The Landau Theory of Phase Transitions* (World Scientific, Singapore, 1987).
[27] S. V. Vonsovsky, Yu. A. Izyumov, and E. Z. Kurmaev, *Superconductivity of Transition Metals* (Springer Verlag, Berlin, 1982).
[28] L. N. Bulaevskii, A. I Buzdin, M. L. Kulić, and S. V. Panyukov, Adv. Phys. 34, 175 (1985); Sov. Phys. Uspekhi, 27, 927 (1984). A. I. Buzdin and L. N. Bulaevskii, Sov. Phys. Uspekhi 29, 412 (1986).
[29] E. I. Blount and C. M. Varma, Phys. Rev. Lett. 42, 1079 (1979).
[30] K. K. Murata and S. Doniach, Phys. Rev. Lett. 29, 285 (1972); G. G. Lonzarich and L. Taillefer, J. Phys. C: Solid State Phys. 18, 4339 (1985); T. Moriya, J. Phys. Soc. Japan 55, 357 (1986); H. Yamada, Phys. Rev. B 47, 11211 (1993).
[31] D. I. Uzunov, *Theory of Critical Phenomena*, Second Edition (World Scientific, Singapore, 2010).
[32] D. V. Shopova and D. I. Uzunov, Phys. Rep. C 379, 1 (2003).
[33] A. A. Abrikosov, Zh. Eksp. Teor. Fiz. 32, 1442 (1957) [Sov. Phys. JETP 5q 1174 (1957)].
[34] E. M. Lifshitz and L. P. Pitaevskii, *Statistical Physics, II Part* (Pergamon Press, London, 1980) [*Landau-Lifshitz Course in Theoretical Physics, Vol. IX*].
[35] H. Belich, O. D. Rodriguez Salmon, D. V. Shopova and D. I. Uzunov, Phys. Lett. A 374, 4161 (2010); H. Belich and D. I. Uzunov, Bulg. J. Phys. 39, 27 (2012).
[36] E. P. Wohlfarth, J. Appl. Phys. 39, 1061 (1968); Physica B&C 91B, 305 (1977).
[37] P. Misra, *Heavy-Fermion Systems*, (Elsevier, Amsterdam, 2008).
[38] K. G. Sandeman, G. G. Lonzarich, and A. J. Schofield, Phys. Rev. Lett. 90, 167005 (2003).
[39] T. F. Smith, J. A. Mydosh, and E. P. Wohlfarth, Phys. rev. Lett. 27, 1732 (1971); G. Oomi, T. Kagayama, K. Nishimura, S. W. Yun, and Y. Onuki, Physica B 206, 515 (1995).
[40] M. Uhlarz, C. Pfleiderer, and S. M. Hayden, Phys. Rev. Lett. 93, 256404 (2004).
[41] D. I. Uzunov, Phys. Rev. B74, 134514 (2006); Europhys. Lett. 77, 20008 (2007).
[42] D. Belitz, T. R. Kirkpatrick, J. Rollbühler, Phys. Rev. Lett. 94, 247205 (2005); G. A. Gehring, Europhys. Lett. 82, 60004 (2008).

[43] B. I. Halperin, T. C. Lubensky, and S. K. Ma, Phys. Rev. Lett. 32, 292 (1974); J-H. Chen, T. C. Lubensky, and D. R. Nelson, *Phys. Rev.* B17, 4274 (1978).
[44] N. Kimura *et al.*, Phys. Rev. Lett. 92 , 197002 (2004).
[45] A. Huxley, I. Sheikin, and D. Braithwaite, Physica B 284-288, 1277 (2000).

IntechOpen